Innovation in monitoring food freeze drying

This is an electronic version (author's version) of an article published in DRYING TECHNOLOGY, Volume 29, Issue 16, pages 1920-1931 (2011).

DRYING TECHNOLOGY is available online at:

http://www.tandfonline.com/openurl?genre=article&issn=0737-3937&volume=29&issue=16&spage=1920

Innovation in monitoring food freeze-drying

Roberto Pisano, Antonello A. Barresi, Davide Fissore

Dipartimento di Scienza dei Materiali e Ingegneria Chimica,
Politecnico di Torino, Torino, Italy

Correspondence: Roberto Pisano, Dipartimento di Scienza dei Materiali e Ingegneria Chimica, Politecnico di Torino, Corso Duca degli Abruzzi 24, 10129 Torino, Italy; E-mail: roberto.pisano@polito.it

Abstract

This paper aims to extend the field of application of the pressure rise technique, from freeze-drying of pharmaceutical or biological products in vials to freeze-drying of liquids or foodstuff in trays. The proposed method, that is based on DPE^{+} algorithm, has been adapted to monitor the drying of liquids in trays and of Individually Quick Frozen products. Examples of results obtained in a small-scale plant wherein such method was used for monitoring the freeze-drying of spinach samples and solutions of sucrose and lactose are presented. Since in bulk freeze-drying the radiant energy coming from the upper shelf might be not negligible, the effectiveness of this method has been tested in presence of different radiating contributions. A more sophisticated algorithm to interpret the pressure rise curve, which uses a mathematical model accounting for both conduction heat transfer from the bottom and radiant energy coming from the upper shelf and including heat accumulation into the dried layer, is proposed and experimentally tested.

Keywords: freeze-drying, monitoring, pressure rise technique, primary drying, food drying

Introduction

In food processing, freeze-drying can be used to preserve highly valuable products whose organoleptic properties can be damaged by the high processing temperature of traditional drying processes, or to make them more convenient for storage and transport. In fact, as the process is carried out at very low temperature, and there is no capillary transport of solutes to the surface, the freeze-dried food retains the aroma, taste and texture of its fresh counterpart, and its porous structure allows fast and good reconstitution.

Products typically processed by freeze-drying can be classified by their original physical state into three basic categories: liquids (like coffee, tea and juices), Individually Quick Frozen (IQF) products (like segments of fruit, vegetables, seafood and meat) and combined ones (like soup blocks, rice dishes and baby foods).[1]

Fundamentally, whichever is the product, the process consists in freezing the material, removing the frozen water by sublimation (primary drying phase) and, finally, further warming of the product to promote moisture desorption.[2]

During freezing, the material is cooled below its triple point. In this step, most of water, that is called “free” water, crystallizes as ice, while the reaming fraction is incorporated into the concentrated solution as “bound” water. A proper design of the freezing stage is fundamental to optimize the successive drying steps, as freezing conditions determine the shape and the size of ice crystals and, thus, the resistance to vapour flow through the dried layer.[3-5] Treatments like annealing (in which product temperature is cycled up and down) can be introduced to get larger ice crystals and, thus, shorten the sublimation step. Size and structure of ice crystals can be also modified, even if only within a limited extent, controlling the cooling and freezing rate, or better, controlling directly the nucleation temperature.[4] Recently, various authors[6-7] proposed alternative methods to induce and control ice nucleation. However, it must be said that the choice of the optimal freezing conditions depends upon product characteristics. For example, large ice crystals are well-liked in case of liquids like coffee extract, since a highly porous matrix, and thus a faster drying and a smaller reconstitution time, is obtained. On the contrary, solid products like food, or objects with formerly-living cells, can be damaged because of cell walls breaking, which results in a poor texture of the rehydrated product.

After freezing, ice is removed as vapour reducing the surrounding pressure and supplying enough heat to allow ice sublimation. During this phase product damages can occurs; thus, it is fundamental to design the process to meet product requirements. In recent

years, the concept of Quality by Design has been applied to pharmaceutical manufacturing[8], but its principles can be also implemented to the drying of food. The application of the concept "Quality by Design" to the primary drying phase often requires coupling opposite needs. For example, product temperature has to be maintained below a specific value to avoid loose of the macroscopic structure, that occurs in case of melting, shrinkage or collapse of the solid matrix.[9] On the contrary, the sublimation rate, and hence product temperature at the moving front, should be maximized to achieve the most cost effective cycle.

In industrial practice, a freeze-drying cycle is specified by means of a recipe, that is the definition of time and processing conditions (i.e. chamber pressure and temperature of the heating shelf) of a sequence of steps. An extended experimental campaign (based on trials and errors) may be required to design this recipe, even if various authors have recently proposed new methods to get it off-line (for example using the design space[10]) or in-line.[11-13] It must be said that these methods were developed for pharmaceutical manufacturing, but can be easily extended to food processing.

The use of a fixed recipe does not guarantee the repeatability of freezing and drying conditions, but, on the other hand, the in-line optimization of the manufacturing process is still limited as the parameters of interest (i.e. product temperature and residual water content) are hardly measurable. However, process constraints are less demanding at laboratory or pilot scale, where a certain margin of freedom is given, allowing the manual insertion of sensors or the introduction of disturbs to identify the process.

In recent years, US Food and Drugs Administration encouraged pharmaceutical manufacturers to use advanced process monitoring techniques.[14] In this context, the design of in-line and non-intrusive tools for process monitoring has received a lot of interest in the literature[15-16] and has been recently reviewed by Refs.[17-18] As methods for recipe developments, these techniques were designed for pharmaceutical manufacturing, since product quality requirements for pharmaceuticals are much more stringent, but there is an increasing interest in extending their use to the drying of food.

The measurement of the moving front temperature and position is only possible with advanced systems. For this purpose, valuable alternatives to the use of thermocouples, like model-based algorithms, have been proposed.

Velardi et al.[19-20] proposed the use of an observer, which combines a priori knowledge of the physical system (mathematical model) with experimental data (e.g. temperature measurements), to provide an almost continuous estimation of the desired variables. Its application in food processing is, however, limited to liquid products, as

thermocouples cannot be easily inserted in pre-frozen products.

Process identification techniques (e.g. the Pressure Rise Test (PRT) technique) can be also used to recover the unknown parameters. These methods are based on the use of a mathematical model to interpret the experimental response of the system (i.e. the pressure rise curve) to a short perturbation, i.e. shut-off of the valve separating the drying and condenser chamber. Among others, the Dynamic Parameters Estimation (DPE), or its upgrade (DPE^+), is one of the tools that have been proposed to monitor the process using the pressure rise curve.[21-22] The monitored variables (i.e. product temperature, heat and mass transfer coefficients and the residual amount of ice) can be then used for closing the loop, enabling an in-line control with a predictive action.[11]

Such devices, however, were designed for monitoring and managing the freeze-drying of pharmaceuticals, mainly liquids in vials. Freeze-drying of foodstuff is, instead, less demanding in terms of control, but during the operation care must still be paid to keep the product temperature lower than its critical value; on the other hand, in case of food processing, it is particularly important to optimize the cycle to reduce its duration and thus the energy consumption, to make it energetically sustainable.

This paper aims to extend the field of application of the PRT technique, from freeze-drying of pharmaceutical and biological products in vials to freeze-drying of liquids and foodstuff in trays. For this purpose, the DPE^+ algorithm (with some upgrades) is used. It will be proven, that, if radiation is limited, the model used in the DPE^+ algorithm can reliably describe the system dynamics, and account for the heat flux due to radiation by considering an effective value for the overall heat transfer coefficient. Instead, if heat is mainly transferred by radiation, the operating principle remains the same, but a different model must be used for the response interpretation: the radiant energy coming from the upper shelf, and the heat accumulation in the dried layer, must be considered in this case.

In the following sections a general description of the pressure rise test technique and of DPE^+ algorithm is given. A particular attention has been reserved to a modified version of DPE^+ algorithm (i.e. DPE^{++}), which also account for the contribution of radiation coming from the upper shelf. Results obtained in a small industrial plant are presented to demonstrate the effectiveness of the proposed approach to monitor and control the freeze-drying of liquids in bulk. The same technique is then used for monitoring the batch freeze-drying of IQF products. The last part of the study instead aims at investigating – by means of numerical simulations and experimental cycles run on purpose– the performances of DPE^+ and DPE^{++} algorithms in presence of different radiating contributions.

Pressure Rise Test technique

The transient pressure response is a process identification technique. In early studies, it was used to determine the completion of ice sublimation[23-24] or, coupled to a relationship for the ice vapour pressure, to estimate the temperature of the product at the moving interface.[25-26] This method was, then, modified by Ref.[27], who proposed to calculate the interface temperature from the value of pressure measured in correspondence of the maximum of the first derivative of the pressure rise curve. In recent years, various authors[21-22, 28-30] proposed to use a mathematical model of the process to estimate the product temperature, as well as other parameters of the system, on the basis of pressure rise data. The various algorithms mainly differ in the type of mathematical model used and parameters estimated.

All these methods do not consider the radiant energy coming from the upper shelf and chamber walls. However, if heat transfer by radiation from walls is limited, it can be accounted simply considering an effective heat transfer coefficient.[22] On the other hand, concerning the radiant energy coming from the upper shelf and the heat accumulation in the dried layer, the relevance of its contribution depends upon the configuration used.[31] This term can be neglected in case of freeze-drying of liquids in vials, where the rubber stopper acts as a shield from radiation. Nevertheless, this assumption is not always acceptable, mainly when liquids are processed in bulk or in containers without stoppers. In this case, as already stated in the introduction, the model used for interpreting the pressure response should be reformulated so that radiation contribution from the upper shelf can be included in the energy balance of the system. In the following sections, the DPE^{+} algorithm, and its modification (DPE^{++}) to include also the radiant contribution, is described in details.

DPE^{+} algorithm

The DPE^{+} algorithm[32] describes the heat transfer and the local evolution of the product temperature in the frozen layer (T_{froz}) during the PRT by means of the following equations:

$$\frac{\partial T_{\text{froz}}}{\partial t} = \frac{k_{\text{froz}}}{\rho_{\text{froz}} c_{p,\text{froz}}} \frac{\partial^2 T_{\text{froz}}}{\partial z^2} \qquad \text{for } t > t_0, \quad L_{\text{dried}} \le z \le L_{\text{tot}} \qquad (1)$$

$$T_{\text{froz}}\Big|_{t=0} = T_{i,0} + \frac{z}{k_{\text{froz}}} \frac{\Delta H_{\text{sub}}}{R_p} \left[p_{\text{ice}} - p_{w,0} \right] \qquad \text{for } L_{\text{dried}} \le z \le L_{\text{tot}} \qquad (2)$$

$$k_{\text{froz}} \left.\frac{\partial T_{\text{froz}}}{\partial z}\right|_{z=L_{\text{dried}}} = \frac{\Delta H_{\text{sub}}}{R_p}\left[p_{\text{ice}} - p_w\right] \qquad \text{for } t \geq t_0, \quad z = L_{\text{dried}} \tag{3}$$

$$k_{\text{froz}} \left.\frac{\partial T_{\text{froz}}}{\partial z}\right|_{z=L_{\text{tot}}} = h\left(T_S - T_B\right) \qquad \text{for } t \geq t_0, \quad z = L_{tot} \tag{4}$$

where z is the axial coordinates ($z = 0$ corresponds to the upper surface of the dried product), $T_i = T_{\text{froz}}\big|_{z=L_{\text{dried}}}$, $T_B = T_{\text{froz}}\big|_{z=L_{tot}}$ and p_{ice} is the equilibrium pressure between ice and vapour. The definition of all the symbols is given in the section at the end of the paper, while a sketch of the physical system (in case of liquid products in tray) is given in Figure 1. The interface of sublimation (at $z=L_{\text{dried}}$) is assumed to be planar and the origin of the z axis is at the product top.

During a pressure rise test, the heat fluxes at $z = L_{\text{dried}}$ and at $z = L_{\text{tot}}$ are not equal, because of accumulation in the frozen layer, but in the beginning they are the same because of the pseudo-stationary hypothesis. Thanks to this assumption, the expression for the heat transfer coefficient, h, can be derived by equating the boundary conditions (3) and (4) at

$$t = t_0: \; h = \left[\frac{T_S - T_{i,0}}{\frac{\Delta H_{\text{sub}}}{R_p}\left(p_{\text{ice}} - p_{w,0}\right)} - \frac{L_{\text{froz}}}{k_{\text{froz}}}\right]^{-1} \tag{5}$$

where $L_{\text{froz}} = L_{\text{tot}} - L_{\text{dried}}$. To calculate the equilibrium vapour pressure, that is a function of the interface temperature, it has been used the equation proposed by Ref.[33], which is recommended by the World Meteorological Organization[34] and whose results are in good agreement with data reported by the International Association for the Properties of Steam[35] and with experimental data reported by Ref.[36]

The dynamics of the water vapour pressure rise is described by the material balance equation for the vapour flowing into the chamber environment. The mass flow rate is expressed as a function of pressure driving force between the product interface and the chamber; thus, applying the ideal gas law, we have:

$$\frac{dp_w}{dt} = \frac{A_{\text{sub}} R T_{\text{gas}}}{V_{DC} M_w R_p}\left(p_{\text{ice}} - p_w\right) \tag{6}$$

Finally, to calculate the total chamber pressure, the constant leakage in the drying chamber (F_{leak}) and the initial partial pressure of inert gases ($p_{in,0}$) has to be known:

$$P_{DC} = p_w + p_{in} = p_w + F_{\text{leak}} \cdot t + p_{in,0} \qquad \text{for } t > t_0 \tag{7}$$

$$p_w\big|_{t=0} = P_{DC,0} - p_{in,0} \qquad \text{for } t > t_0 \tag{8}$$

The actual thickness of the frozen layer is determined through a material balance written across the moving interface, which is solved together with the previous equations. Integrating the material balance at the interface between the previous and the current PRT, it follows:

$$L_{\text{froz}} = L_{\text{froz}}^{(-1)} - \frac{1}{\rho_{\text{ice}} - \rho_{\text{dried}}} \int_{t_0^{(-1)}}^{t_0} \frac{1}{R_p}\left(p_{\text{ice}} - p_w\right) dt \tag{9}$$

Once the pressure rise curve has been acquired, the sublimation rate (at the time t_j during a PRT) can be calculated without using any model, but only evaluating the slope of the pressure rise curve[21, 37]:

$$J_w\big|_{t=t_j} = \frac{V_{DC} M_w}{A_{\text{sub}} R T_{\text{gas}}} \left.\frac{dp_w}{dt}\right|_{t=t_j} \qquad \text{for } t > t_0 \tag{10}$$

To calculate the first derivative of the pressure rise curve at $t = t_j$, a natural cubic spline is used for fitting the experimental data and the first derivative of the interpolated function is approximated with the first derivative of the spline. Then, the flow rate of water vapour can be calculated, provided that the value of T_{gas} is known. If the temperature of the chamber gas is not available, it can be substituted with the value of the product temperature at the moving front, usually committing a small error.[21]

Combining Equations (6) and (10), the resistance to mass transfer can be expressed as a function of the initial slope of the curve of pressure rise, T_{gas} and T_i, as shown in the following:

$$R_p = \left(\frac{A_{\text{sub}} R T_{\text{gas}}}{V_{DC} M_w}\right)\left(\left.\frac{dp_w}{dt}\right|_{t=t_0}\right)^{-1}\left(p_{\text{ice}} - p_{w,0}\right) \tag{11}$$

According to Equation (11), once the pressure rise curve has been acquired and its initial slope has been calculated, the value of R_p depends only on $T_{i,0}$. Hence, if the value of the front temperature is somehow estimated, the value of R_p is known. Thus $T_{i,0}$ is the only model parameter that must be estimated for interpreting the pressure response. The steps of the optimization procedure are summarized below:

(1) initial guess of $T_{i,0}$;

(2) calculation of the first derivative of the pressure rise curve at $t = t_0$ and, then, of R_p

using Equation (11);

(3) calculation of L_{froz} according to Equation (9);

(4) determination of the effective overall heat transfer coefficient h and of the initial temperature profile using Equation (2) and (5);

(5) integration of the system of algebraic and differential equations that describes the pressure rise in the interval (t_0, t_f), thus calculating P_{DC};

(6) determination of the optimal value of $T_{i,0}$ that best fits the simulated chamber pressure and the measured values.

DPE^{++} algorithm

To monitor the primary drying phase in presence of high radiation, the mathematical model used to describe process dynamics during a pressure rise test has to account for the radiant energy coming from the upper shelf and the heat accumulation in the dried layer. For this purpose, the mathematical model has to include the energy balance equation for the dried layer, besides the balance for the frozen product (see Equations (1) and (4)).

The dried layer (that is comprised of the solid product and gas flowing through it) is considered as a pseudo-homogenous system and is described by effective properties that account for the contribution of the two phases. The evolution of product temperature along the dried layer (T_{dried}) is, thus, described by the following equations:

$$\frac{\partial T_{\text{dried}}}{\partial t} = \frac{k_{\text{dried},e}}{\rho_{\text{dried},e} c_{p,\text{dried},e}} \frac{\partial^2 T_{\text{dried}}}{\partial z^2} - \frac{c_{p,\text{gas}} J_w}{\rho_{\text{dried},e} c_{p,\text{dried},e}} \frac{\partial T_{\text{dried}}}{\partial z} \qquad \text{for } t > t_0, \quad 0 \le z \le L_{\text{dried}} \tag{12}$$

$$T_{\text{dried}}\Big|_{t=0} = T_{\text{dried},0}\Big|_{z=0} \times \left(1 - \frac{c_{p,\text{gas}} J_w}{k_{\text{dried},e}} z\right) \times e^{\frac{c_{p,\text{gas}} J_w}{k_{\text{dried},e}} z} \qquad \text{for } 0 \le z \le L_{\text{dried}} \tag{13}$$

$$-k_{\text{dried},e} \frac{\partial T_{\text{dried}}}{\partial z}\bigg|_{z=0} = \sigma \varepsilon F \left(T_S^4 - T_{\text{dried}}\Big|_{z=0}^4\right) \qquad \text{for } t \ge t_0, \quad z = 0 \tag{14}$$

$$k_{\text{froz}} \frac{\partial T_{\text{froz}}}{\partial z}\bigg|_{z=L_{\text{dried}}} - k_{\text{dried},e} \frac{\partial T_{\text{dried}}}{\partial z}\bigg|_{z=L_{\text{dried}}} = \frac{\Delta H_{\text{sub}}}{R_p}\left(p_{\text{ice}} - p_w\right) \qquad \text{for } t \ge t_0, \quad z = L_{\text{dried}} \tag{15}$$

To get Equation (12), we have assumed that the gas flow rate along the dried layer is constant and equal to J_w. Equation (13), instead, is obtained by Equation (12) assuming steady-state conditions. In addition, the initial condition of Equation (2) and the boundary condition of

Equation (3) have to be modified:

$$T_{\text{froz}}\Big|_{t=0} = T_{i,0} + \frac{z}{k_{\text{froz}}}\left[\frac{\Delta H_{\text{sub}}}{R_p}\left(p_{\text{ice},0} - p_{w,0}\right) - \sigma\varepsilon F\left(T_S^4 - T_{\text{dried},0}\Big|_{z=0}^4\right)\right]$$

$$\text{for } L_{\text{dried}} < z \le L_{\text{tot}} \tag{16}$$

$$k_{\text{froz}}\frac{\partial T_{\text{froz}}}{\partial z}\Bigg|_{z=L_{\text{dried}}} = \frac{\Delta H_{\text{sub}}}{R_p}\left[p_{\text{ice}}\left(T_i\right) - p_w\right] - \sigma\varepsilon F\left(T_S^4 - T_{\text{dried},0}\Big|_{z=0}^4\right)$$

$$\text{for } t \ge t_0, \quad z = L_{\text{dried}} \tag{17}$$

Furthermore, Equation (5) that gives the overall heat transfer coefficient h, which compares in Equation (4), is substituted by:

$$h = \left[\frac{T_S - T_{i,0}}{\frac{\Delta H_{\text{sub}}}{R_p}\left(p_{\text{ice}}\left(T_{i,0}\right) - p_{w,0}\right) - \sigma\varepsilon F\left(T_S^4 - T_{\text{dried},0}\Big|_{z=0}^4\right)} - \frac{L_{\text{froz}}}{k_{\text{froz}}}\right]^{-1} \tag{18}$$

The transient pressure rise curve is still described by Equations (6), (7) and (8); however, in this case the model parameter that must be estimated for interpreting the pressure response is the product temperature at the top surface, that is $T_{dried}\big|_{z=0}$, thus the optimization procedure has to be modified as described in the following:

(1) initial guess of $T_{\text{dried}}\big|_{z=0}$;

(2) calculation of the first derivative of the pressure rise curve at $t = t_0$ and of J_w using Equation (10);

(3) calculation of $T_{i,0}$ using Equations (13) and (16) and, then, of R_p using Equation (11);

(4) calculation of L_{froz} according to Equation (9);

(5) determination of the effective overall heat transfer coefficient h using Equation (18);

(6) integration of the system of algebraic and differential equations that describes the pressure rise in the interval (t_0, t_f), thus calculating P_{DC};

(7) determination of the optimal value of $T_{\text{dried}}\big|_{z=0}$ that best fits the simulated chamber pressure and the measured values.

Material and Methods

Equipment and Instrumentation

Results discussed in this paper have been obtained in a small-size industrial apparatus (*LyoBeta* 25™ by Telstar, Terrassa, Spain) with a chamber volume of 0.2 m^3 and equipped with T-type miniature thermocouples (by Tersid S.p.A., Milano, Italy), capacitance (Baratron type 626A, by MKS Instruments, Andover, MA, USA) and thermal conductivity (Pirani type PSG-101-S, by Inficon, Bad Ragaz, Switzerland) gauges. The pressure in the drying chamber is regulated by bleeding of inert gas, whose flow rate is measured through a mass flow meter (type MB100, BY MKS Instruments, Andover, MA, USA). Of course, the controlled leakage valve is closed during a pressure rise test. The apparatus is equipped with *LyoMonitor*[17], a system that allows for process monitoring using various devices, and *LyoDriver*[11] for process control.

Materials

Experiments were carried out using aqueous solution of sucrose (Riedel de Haën) and lactose (Ardetfarma). All reagents were analytical grade and used as received. Solutions were prepared using ultra-pure water (Milli-Q RG, Millipore, Billerica, MA) and poured into stainless steel trays. A further test was carried out using pre-frozen bleached spinach samples pressed in cubes with a weight of about 60 g each.

Experimental Planning

In case of bulk freeze-drying of liquids, the freezing phase was carried out at 223 K for about 5 h. During the primary drying phase, chamber pressure was reduced to 10 or 20 Pa, while a different value of shelf temperature (T_S) was set for the various tests to study the effectiveness of DPE$^+$ algorithms to monitor systems with a different contribution of the radiative heat coming from the upper shelf. Thus, the following tests were carried out:

(1) Bulk freeze-drying of a liquid solution of sucrose (10% by weight) in case of moderate upper shelf radiation (T_S =253 K, P_{DC} =20 Pa);

(2) Bulk freeze-drying of a liquid solution of lactose (5% by weight) in case of stronger radiation (T_S =273 K, P_{DC} =10 Pa);

(3) Bulk freeze-drying of an IQF product (e.g. spinaches) in case of moderate upper shelf radiation (T_S =263 K, P_{DC} =10 Pa).

Protocol of validation

The adequacy of the model-based tool (DPE^+) to monitor the dynamics of the product was tested considering the total drying time and product temperature response. In particular, the completion of the sublimation was determined monitoring the following process parameters:

- The frozen layer thickness;
- The product temperature that can be continuously monitored by thermocouples;
- The composition of chamber gas that is estimated by comparison between pressure signals supplied by Baratron and Pirani sensors.

On the other hand, the time evolution of the product temperature – at the bottom – predicted by DPE^+ and DPE^{++} algorithms is validated upon comparison with experimental values obtained through miniature thermocouples, at least until their readings are reliable (as it will be discussed afterwards, the insertion of probes into the product can alter its drying kinetics).

Results

An example of freeze-drying cycle where the pressure rise technique, coupled with DPE^+ algorithm, is used for monitoring the primary drying stage of a liquid (i.e. a 10% by weight sucrose solution) in trays is illustrated in Figure 2. The drying was carried out at constant chamber pressure and shelf temperature. Operating conditions were chosen so that the contribution of the radiative energy (coming from the upper shelf) is much smaller than the heat transferred by conduction from the lower shelf: approximately the radiant heat was 15% of the total heat transferred to the product. In particular, the drying was carried out at low T_S (=253 K) and a relatively high value of P_{DC} (=20 Pa).

The adequacy of the DPE^+ method to describe the dynamics of the product was tested upon two process parameters: the product temperature at the container bottom and the duration of the primary drying. Concerning the former, DPE^+ estimations were compared with values measured through various thermocouples, which were inserted into the product and in close contact with the bottom of the container. It must be remarked that DPE^+ can estimate the entire temperature profile along the frozen layer; nevertheless, to facilitate the positioning of temperature sensors, the comparison between the product temperature estimated by DPE^+ algorithm and measured by thermocouples is limited to the value observed at the container bottom. Figure 2 (upper graph) shows a good agreement between experimental measurements

and DPE^{+} estimations, at least until ice was still present nearby the probe. In fact, at the end of the primary drying product temperature sharply increases, because the heat supplied by the shelf is no longer used to sublimate ice, but to heat the product. Nevertheless, thermocouples can alter the process of nucleation and ice crystals growth in the zone around the sensor probe, which can be also responsible for an increased heat transfer, determining a lower resistance to vapour flow and, thus, a higher drying rate. It follows that, if the drying time is derived from the product temperature response, the result can be misleading.[24] A more reliable way to detect the completion of ice sublimation is monitoring the gas composition in the drying chamber, for example comparing the pressure reading obtained by a capacitance and a thermal conductivity manometer.[38] In fact, the concentration of water in the drying chamber becomes very low when the drying finishes, thus Pirani and Baratron sensors measure almost the same value of pressure and their ratio becomes equal to one. In this study, the completion of the sublimation was associated with the starting point of the decreasing part of the pressure ratio curve. In fact, the time required by the system to pass from high water content to only inert gas depends on the operating conditions considered and batch properties.[39-40] The consequence is that the evolution of chamber gas composition nearby the endpoint can vary with the cycle set-up, loading and product type.

Beside product temperature, the DPE^{+} algorithm can also estimate the position of the moving front and, hence, the thickness of the frozen layer. This information can be used to estimate the end of the sublimation as the time at which L_{froz} is equal to zero. Figure 2 (lower graph) shows a good agreement between the drying time experimentally measured by pressure ratio and estimated by DPE^{+}. Figure 2 also compares the values of T_B and L_{froz} vs. time estimated by DPE^{+} and DPE^{++} algorithms. As the cycle is carried out under moderate radiation from the environment, the outcomes of the two algorithms are in good agreement.

Once it has been proved that DPE^{+} and DPE^{++} can reliably monitor the drying of liquids in bulk, the algorithms were used for monitoring the freeze-drying of IQF products. Even in this case, the operating conditions were chosen so that radiation from the upper shelf is not very relevant (about 15% of the total heat transferred to the product). Figure 3 shows the results that can be obtained in a freeze-drying cycle, wherein spinach samples were considered as test product. The operating conditions used for the primary drying phase are displayed in graph (a). The temperature of the product was measured – at various positions inside the sample, but always at the bottom of the product – through miniature thermocouples (see Figure 3, graph c) and regularly estimated through DPE^{+} and DPE^{++} algorithms. As far as

measurements obtained through thermocouples are concerned, a good agreement with DPE^{+}/DPE^{++} predictions is obtained in terms of temperature at the bottom of the product cube. Nevertheless, it must be evidenced that temperature measurements can be considered reliable only in the first part of the drying (until 10 hours), then they suddenly increased up to the shelf value: this is an indication that ice surrounding the probe was sublimated. These data confirm that the portion of the product in contact with the temperature sensors underwent a faster drying kinetics. This behaviour might be due to the fact that the insertion of the sensor probe in pre-frozen product is quite invasive and can create preferential paths for the vapour flow. The evolution of pressure ratio is illustrated in graph (a). Graph (b) instead, displays the value of L_{froz} vs. time estimated by DPE^{+}/DPE^{++} algorithm. As indicated by the change of the composition in the chamber (see pressure ratio curve in graph a), the sublimation step was completed after about 135 hours, and this was confirmed by pressure rise test results: the frozen layer thickness is, in fact, reduced to almost zero nearby such time. It is worth noticing that the very long drying time is a consequence of samples size and process conditions selected to reduce radiating effects.

The last part of this study aims at investigating the performances of DPE^{+} algorithm to monitor a process in bulk, but in presence of different radiating contributions. Results obtained using DPE^{+} and DPE^{++} are also compared.

As first attempt, we have used a detailed model of the process to predict the process dynamics, in case of bulk freeze-drying of liquids, when the drying is carried out using different values of shelf temperature. For this purpose, the detailed mathematical model proposed by Ref.[41] has been used; the mono-dimensional one, without the effect of the container wall, is well suited for the case of bulk freeze-drying of liquids in trays. In this manner, we can study the effectiveness of DPE^{+} tool to monitor the drying when different contributions of the upper shelf radiation to the heat balance are involved, without introducing other sources of variability. Regular pressure rise curves (one every 30 minutes) were also simulated and a sampling frequency of 10 Hz is assumed. The case study that is analyzed is the freeze-drying of a generic solution (10% by weight solute content), processed in a metal tray with an internal diameter of 229 mm (L_{tot}=10.3 mm, P_{DC}=10 Pa and V_{DC}=0.175 m^3). The product structure is assumed to be homogeneous (constant porosity along the dried layer and no crust formation), thus a linear dependence of R_p upon the thickness of the dried layer can be used. Side-radiation coming from chamber walls is not considered, so the role of only upper shelf radiation on DPE^{+} performances can be better investigated.

An example of product dynamics that can be obtained considering two different temperatures of the heating shelves is given in Figure 4 and 5. Figure 4 compares the system dynamics – in terms of product temperature and front position – simulated by the detailed model and estimated by DPE$^+$ algorithm in case of moderate product heating (T_S =243 K). It can be observed that DPE$^+$ can accurately estimate both the temperature at the interface and at the product bottom, as well as the state of progress of the drying.

When the product is processed at a higher temperature of the shelf (see Figure 5), DPE$^+$ algorithm accounts for the higher heat flux due to radiation by considering an effective heat transfer coefficient and, thus, overestimated the parameter h: the estimated value was 20 W m^{-2} K^{-1}, while the value used to carry out the simulation was 15 W m^{-2} K^{-1}. Besides that, the algorithm slightly underestimated the temperature of the frozen product. Nevertheless, even if the contribution of the radiating heat from the upper shelf is much more significant, DPE$^+$ can still estimate satisfactorily the duration of the drying (see Figure 5). It follows that DPE$^+$ algorithm can effectively be used to monitor the state of progress of the drying even in presence of a high radiating heat from the upper shelf, conditions that are common in food processing, but caution must be paid on the estimation of all the other parameters, e.g. the temperature of the frozen product.

It must be remarked that if the heat is mainly transferred by radiating the product from the upper shelf, the temperature profile along the product might be reversed: the temperature at the moving interface is higher than that at the bottom because of heat accumulation in the dried layer. In such conditions, it is fundamental including the enthalpy balance of the dried cake in the formulation of the algorithm. Figure 6 shows an example of results that can be obtained in case the heat is mainly transferred by radiation from the upper shelf. Such results have been obtained assuming a very high resistance to heat transfer at product bottom. In this case, as expected, the product temperature along the frozen layer is reversed: the value of temperature is higher at the interface than at the bottom (see graph b). However, even if DPE$^+$ significantly underestimates the product temperature (see graph c), it can be still used for monitoring the state of progress of the sublimation: a good agreement between the drying time estimated by DPE$^+$ algorithm and calculated by the model can be observed (see graph a). In fact, the calculation of the mass flow rate of water vapour is obtained from the initial slope of the pressure rise curve, thus is less affected by model assumptions concerning the enthalpy balance. Furthermore, even if its calculation involves the DPE$^+$ estimation of T_i (see Equation (11)), a large uncertainty upon the product temperature (e.g. 10 K) has a small effect

on the final value of J_w (<5%). In this case, to get a reliable and effective estimation of the product temperature, DPE^{++} algorithm has to be used: in graphs (a) and (c), a good agreement between model predictions and DPE^{++} estimations, in terms of position and temperature of the moving interface, can be observed for the entire primary drying phase.

A final issue concerns the role of side-walls radiation. It can affect the heat flux to the samples, increase the sublimation rate and hence modify the temperature profile along the frozen layer, which cannot be assumed linear anymore; the direct consequence of this is the reduction of the sublimating area towards the end of the main drying stage. Despite that, if radiating heat is limited, also in this case it can be accounted for by simply defining an effective heat transfer coefficient[22] and, since only a small fraction of product is radiated, which is the part located laterally, DPE^{+} algorithm can compensate this lack of the model estimating an average state of the system. On the contrary, if the radiating heat is significant, deviations in temperature profile become relevant and DPE^{+} results might be not representative of the real product dynamics.

It follows that if heat is mainly transferred by radiation, whichever is the source, DPE^{+} cannot predict correctly the temperature of the product, and a more complex model that also takes into account heat accumulation in the dried layer must be used. Figure 7 shows an example of freeze-drying cycle where the pressure rise technique, coupled with DPE^{+}/DPE^{++} algorithms, is used for monitoring the primary drying stage of a liquid in trays (i.e. a 10% by weight lactose solution) in case the contribution of radiative energy coming from the upper shelf (T_S =273 K) is much more relevant (about 30% of the total heat transferred to the product). The temperature of the product estimated by pressure rise technique and measured through thermocouples is displayed in graph a. As a further confirmation of previous discussion based on model simulations, DPE^{+} algorithm did not estimate correctly the value of T_B . On the contrary, the estimation of product temperature obtained by DPE^{++} algorithm, which is based on a mathematical model accounting for radiant energy coming from the upper shelf and heat accumulation in the dried layer, fairly agreed with experimental evidences. Unfortunately, thermocouples allows monitoring only the product temperature in a fixed point, usually at the bottom or at the centre of the sample, while the temperature profile along the entire frozen layer is not given. In some cases, in particular when the radiation from the upper shelf is very relevant, the temperature of the product is higher at the moving front, not at the bottom as typically happens when heat is supplied only through the shelf. In this case information supplied by thermocouples is not exhaustive since the position of the sublimation

front changes during the drying and hence thermocouples cannot measure its temperature. However, it is worth restating that, unlike product temperature estimation, both algorithms could predict correctly the evolution of J_w vs. time (see Figure 7, lower graph). In particular, in correspondence of the primary drying end-point, that was detected by pressure ratio analysis, the value of vapour flow estimated by pressure rise technique tends to zero.

Conclusions

The feasibility of using the DPE^+ algorithm for monitoring the sublimation step of a freeze-drying cycle applied to liquids or IQF products in trays has been discussed. In particular, it has been proved that the pressure rise technique, coupled with DPE^+ algorithm, can be effectively used for monitoring both the product temperature and the state of progress of the drying only if the radiant energy coming from the upper shelf is limited. However, it has been observed that, even in presence of significant radiation from the upper shelf, DPE^+ can be still used to evaluate the mass flow rate of water vapour and hence the completion of the sublimation step.

In case the PRT technique is used for monitoring the primary drying phase in presence of high radiation, the model used has to account for the radiant energy coming from the upper shelf and the heat accumulation in the dried layer. For this purpose, a modified algorithm to interpret the pressure rise curve, that is DPE^{++} algorithm, has been here proposed and validated. It has been proven that DPE^{++} can be effectively used for monitoring the bulk freeze-drying of foodstuff even in case the radiant heat coming from the upper shelf is relevant. However, in this work all the tests were carried out in trays loaded on heating shelves, where the heat is mainly transferred by conduction from the lower shelf. On the contrary, the case wherein the heat transferred by radiation is predominant (e.g. let consider the case wherein the tray is suspended between the lower and upper shelves) needs a further investigation.

It must be said that it is not possible to identify a cutoff value over which DPE^+ results are misleading. Nevertheless, in this study it has been observed that DPE^+ algorithm can effectively monitor the product temperature if the radiative heat contribution is lower than 15% of the total heat transferred to the product. Beyond this limit, the estimation of product temperature worsen, as the fraction of heat transferred by radiation increases, and the use

DPE^{++} algorithm is strongly recommended.

Finally, it must be remarked that the pressure rise technique is suitable for monitoring the food manufacturing in batch; in case the production plant is continuous, the process might be monitored by software sensors – similar to those developed for freeze-drying of liquids in vials – eventually coupled with wireless temperature sensors.

Nomenclature

A_{sub}	sublimation area, m^2
c_p	specific heat, J $kg^{-1}K^{-1}$
F	view factor for radiative heat transfer
F_{leak}	leakage rate, Pa s^{-1}
h	heat transfer coefficient from the shelf to the product, W m^{-2} K^{-1}
ΔH_{sub}	heat of sublimation, J kg^{-1}
J	sublimation flux, kg s^{-1} m^{-2}
k	thermal conductivity, W m^{-1} K^{-1}
L	product thickness, m
M_w	molar mass of water, kg $kmol^{-1}$
p	partial pressure inside the drying chamber, Pa
p_{ice}	vapour pressure at the sublimation interface, Pa
P_{DC}	total pressure inside the drying chamber, Pa
R	ideal gas constant, J K^{-1} mol^{-1}
R_p	mass transfer resistance in dried layer, m s^{-1}
t	time, s
T	temperature, K
V_{DC}	volume of the drying chamber, m^3
z	axial coordinate, m

Greek letters

ε	emissivity
ρ	mass density, kg m^{-3}
σ	Boltzmann constant, W $m^{-2}K^{-4}$

Subscripts and superscripts

0	at the beginning of the PRT
(-1)	PRT before the current one
B	at product bottom

dried	dried layer
e	effective
f	at the end of the PRT
froz	frozen layer
gas	chamber gas
i	at moving front position
in	inert gas
S	heating shelf
tot	total
w	water vapour

Abbreviations

DPE	Dynamic Parameters Estimation
IQF	Individually Quick Frozen products
PRT	Pressure Rise Technique

References

(1) Fissore, D.; Barresi, A. A.; Freeze-drying equipments and processing conditions. In Operations in Food Refrigeration; Mascheroni, R. H. Ed.; CRC Press Inc. - Taylor & Francis Group: Boca Raton, FL (USA), 2011.

(2) Gibert, H.; Boeh-Ocansey, O. A study of the primary phase of food freeze-drying in vacuo. Drying Technology 1985, 3 (3), 349-372.

(3) Patapoff, T. W.; Overcashier, D. E. The importance of freezing on lyophilization cycle development. BioPharm International 2002, 15 (3), 16-21.

(4) Hottot, A.; Vessot, S.; Andrieu, J. A direct characterization method of the ice morphology. Relationship between mean crystals size and primary drying times of freeze-drying processes. Drying Technology 2004, 22 (8), 2009-2021.

(5) Marques, L. G.; Freire, J. T. Analysis of freeze-drying of tropical fruits. Drying Technology 2005, 23 (9), 2169-2184.

(6) Gasteyer, T. H.; Sever, R. R.; Hunek, B.; Grinter, N.; Verdone, M. L. Method of inducing nucleation of a material. United States patent US 2007/0186567 A1, 2007.

(7) Patel, S. M.; Bhugra, C.; Pikal, M. J. Reduced pressure ice fog technique for controlled ice nucleation during freeze-drying. AAPS PharmSciTech 2009, 10 (4), 1406-1411.

(8) Rathore, A. S.; Winkle, H. Quality by design for biopharmaceuticals. Nature Biotechnology 2009, 27 (1), 26-34.

(9) Bhandari, B. R.; Howes, T. Implication of glass transition for the drying and stability of dried foods. Journal of Food Engineering 1999, 40 (1-2), 71-79.

(10) Giordano, A.; Barresi, A. A.; Fissore, D. On the use of mathematical models to build the design space for the primary drying phase of a pharmaceutical lyophilization process. Journal of Pharmaceutical Sciences 2011, 100 (1), 311-324.

(11) Pisano, R.; Fissore, D.; Velardi, S. A.; Barresi, A. A. In-line optimization and control of an industrial freeze-drying process for pharmaceuticals. Journal of Pharmaceutical Sciences 2010, 99 (11), 4691-4709.

(12) Tang, X. C.; Nail, S. L.; Pikal, M. J. Freeze-drying process design by manometric temperature measurement: design of a smart freeze-dryer. Pharmaceutical Research 2005, 22 (4), 685-700.

(13) Gieseler, H.; Kramer, T.; Pikal, M. J. Use of manometric temperature measurement (MTM) and SMART™ freeze dryer technology for development of an optimized freeze-

drying cycle. Journal of Pharmaceutical Sciences 2007, 96 (12), 3402-3418.

(14) US Food and Drug Administration. PAT guidance for industry – a framework for innovative pharmaceutical development, manufacturing and quality assurance (US Department of Health and Human Services, Food and Drug Administration, Center for drug evaluation and research, Center for veterinary medicine, Office of regulatory affairs, Rockville, MD, September, 2004).

(15) Fissore, D.; Pisano, R.; Rasetto, V.; Marchisio, D. L.; Barresi, A. A.; Vallan, A.; Corbellini, S. Applying Process Analytical Technology (PAT) to lyophilization processes. Chimica Oggi-Chemistry Today 2009, 27 (2, Supplement), vii-xi.

(16) Wiggenhorn, M.; Presser, I.; Winter, G. The current state of PAT in freeze-drying. American Pharmaceutical Review 2005, 8 (1), 38-44.

(17) Barresi, A. A.; Pisano, R.; Fissore, D.; Rasetto, V.; Velardi, S. A.; Vallan, A.; Parvis, M.; Galan, M. Monitoring of the primary drying of a lyophilization process in vials. Chemical Engineering and Processing 2009, 48 (1), 408-423.

(18) Barresi, A. A.; Velardi, S. A.; Pisano, R.; Rasetto, V.; Vallan, A.; Galan, M. In-line control of the lyophilization process. A gentle PAT approach using software sensors. International Journal of Refrigeration 2009, 32 (5), 1003-1014.

(19) Velardi, S. A.; Hammouri, H.; Barresi, A. A. In-line monitoring of the primary drying phase of the freeze-drying process in vial by means of a Kalman filter based observer. Chemical Engineering Research and Design 2009, 87 (10), 1409-1419.

(20) Velardi, S. A.; Hammouri, H.; Barresi, A. A. Development of a High Gain observer for in-line monitoring of sublimation in vial freeze drying. Drying Technology 2010, 28 (2), 256-268.

(21) Fissore, D.; Pisano, R.; Barresi, A. A. On the methods based on the pressure rise test for monitoring a freeze-drying process. Drying Technology 2011, 29 (1), 73-90.

(22) Velardi, S. A.; Rasetto, V.; Barresi, A. A. Dynamic Parameters Estimation method: advanced Manometric Temperature Measurement approach for freeze-drying monitoring of pharmaceutical solutions. Industrial & Engineering Chemistry Research 2008, 47 (21), 8445-8457.

(23) Neumann, K. H. Freeze-drying apparatus. United States patent US 2994132, 1961.

(24) Nail, S. L.; Johnson, W. Methodology for in-process determination of residual water in freeze-dried products. Developments in Biological Standardization 1992, 74, 137-151.

(25) Oetjen, G. W.; Ehlers, H.; Hackenberg, U.; Moll, J.; Neumann, K. H.; Temperature measurement and control of freeze-drying processes. In Freeze-Drying of Foods; Fisher, F. R.

Ed.; National Academy of Sciences - National Research Council: Washington, D. C., USA., 1962.

(26) Willemer, H. Measurements of temperatures, ice evaporation rates and residual moisture contents in freeze-drying. Developments in Biological Standardization 1992, 74 (4), 123-136.

(27) Oetjen, G. W.; Haseley, P.; Klutsch, H.; Leineweber, M. Method for controlling a freeze-drying process. United States patent US 6163979, 2000.

(28) Milton, N.; Pikal, M. J.; Roy, M. L.; Nail, S. L. Evaluation of manometric temperature measurement as a method of monitoring product temperature during lyophilization. PDA Journal of Pharmaceutical Science and Technology 1997, 51 (1), 7-16.

(29) Liapis, A. I.; Sadikoglu, H. Dynamic pressure rise in the drying chamber as a remote sensing method for monitoring the temperature of the product during the primary drying stage of freeze-drying. Drying Technology 1998, 16 (6), 1153-1171.

(30) Chouvenc, P.; Vessot, S.; Andrieu, J.; Vacus, P. Optimization of the freeze-drying cycle: a new model for pressure rise analysis. Drying Technology 2004, 22 (7), 1577-1601.

(31) Jafar, F.; Farid, M. Analysis of heat and mass transfer in freeze drying. Drying Technology 2003, 21 (2), 249-263.

(32) Fissore, D.; Pisano, R.; Barresi, A. A. Method for monitoring primary drying of a freeze-drying process. International patent PCT/IB2010/056011, 2010.

(33) Goff, J. A.; Gratch, S. Low-pressure properties of water from -160 to 212 °F. Transactions of the American Society of Heating and Ventilating Engineers. Proceedings of 52nd Annual Meeting of the American Society of Heating and Ventilating Engineers, New York, 1946; 95-122.

(34) Vömel, H.; Saturation vapor pressure formulations. Available at: http://cires.colorado.edu/~voemel/vp.html (accessed Mar 2011)

(35) Wagner, W.; Saul, A.; Pruss, A. International equations for the pressure along the melting and along the sublimation curve of ordinary water substance. Journal of Physical and Chemical Reference Data 1994, 23 (3), 515-527.

(36) Marti, J.; Mauersberger, K. A survey and new measurements of ice vapor pressure at temperatures between 170 and 250 K. Geophysical Research Letters 1993, 20 (5), 363-366.

(37) Oetjen, G.-W. Freeze-Drying; Wiley-VCH Verlag; Weinheim, 1999.

(38) Armstrong, J. G. Use of the capacitance manometer gauge in vacuum freeze-drying. Journal of the Parenteral Drug Association 1980, 34 (6), 473-483.

(39) Patel, S. M.; Doen, T.; Pikal, M. J. Determination of end point of primary drying in

freeze-drying process control. AAPS PharmSciTech 2010, 11 (1), 73-84.
(40) Pisano, R.; Guler, B. S.; Barresi, A. A. In-line detection of endpoint of sublimation in a freeze-drying process. Proceedings of European Drying Conference AFSIA 2009, Lyon, 14-15 May, 2009; Cahier de l'AFSIA Nr 23, AFSIA-ESCPE; 110-111.
(41) Velardi, S. A.; Barresi, A. A. Development of simplified models for the freeze-drying process and investigation of the optimal operating conditions. Chemical Engineering Research & Design 2008, 86 (A1), 9-22.

List of Figures

Figure 1. Sketch of a freeze-drying process during the sublimation phase.

Figure 2. Freeze-drying of a sucrose solution (10% by weight) carried out in bulk, in a circular metal tray ($L_{froz,0}$=10.3 mm). (Upper graph): product temperature measured by some thermocouples (dashed line) and estimated by pressure rise technique coupled with DPE^{+} (○) and DPE^{++} algorithm (×). The temperature of the heating shelf (solid line) and Pirani-Baratron pressure ratio (solid line, right-side axis) are also displayed. (Lower graph) Estimations of the frozen layer thickness obtained by PRT technique. The completion of sublimation is also evidenced (vertical dashed line).

Figure 3. Freeze-drying of spinaches: cycle run using 32 samples having an almost cubic shape, with a side of 44 mm, and a total weight of 1.935 kg. (Graph a): time evolution of shelf temperature (solid line), pressure ratio and product temperature estimated by pressure rise technique coupled with DPE^{+} (○) and DPE^{++} algorithm (×). (Graph b) Estimations of the frozen layer thickness obtained by PRT technique. (Graph c) Temperature evolution of the shelf (solid line) and product measured by thermocouples (dashed line) and estimated by pressure rise technique (symbols). The completion of sublimation is also displayed (vertical dashed line).

Figure 4. Example of application of DPE^{+} algorithm for monitoring the freeze-drying of liquids in bulk. The primary drying phase is carried out at P_{DC}=10 Pa and T_S =243 K. (Upper graph): time evolution of T_i calculated by the detailed model (solid line) and estimated through DPE^{+} algorithm (○); T_B : calculated by detailed model (dashed line) and estimated by DPE^{+} (▲). (Lower graph) frozen layer thickness estimated through DPE+ algorithm (○) and given by the model (solid line).

Figure 5. Example of application of DPE^{+} algorithm for monitoring the freeze-drying of liquids in bulk. The primary drying phase is carried out at P_{DC}=10 Pa and T_S =303 K. (Upper graph): time evolution of T_i calculated by the detailed model (solid line) and estimated through DPE^{+} algorithm (○); T_B : calculated by detailed model (dashed line) and estimated by

DPE^+ (▲). (Lower graph): frozen layer thickness estimated through DPE+ algorithm (○) and given by the model (solid line).

Figure 6. Example of application of DPE^+ algorithm to monitor the freeze-drying of liquids in bulk in case the heat is mainly transferred by radiation. (Graph a): frozen layer thickness estimated by DPE^+ algorithm (○) and calculated by the model (solid line). (Graph b): product temperature profile calculated by the model after 5 hours of drying. (Graph c): interface temperature calculated by the detailed model (solid line) and estimated through DPE^+ algorithm (○). Results obtained by DPE^{++} algorithm (×) are also displayed in graph (a) and (c).

Figure 7. Bulk freeze-drying of a lactose solution (5% by weight) carried out in metal trays ($L_{froz,0}$=26 mm) at T_S =273 K and P_{DC} =10 Pa. (Upper graph): product temperature measured by thermocouples (dashed line) and estimated by pressure rise technique coupled with DPE^+ (○) and DPE^{++} algorithm (×). The temperature of the heating shelf and Pirani-Baratron pressure ratio are also displayed. (Lower graph): Estimations of the frozen layer thickness obtained by PRT technique. The completion of sublimation is also evidenced (vertical dashed line).

Figure 1

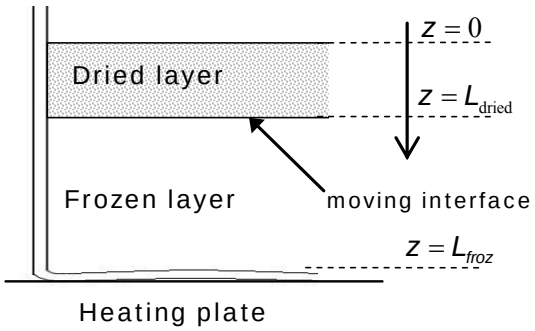
$z = 0$
Dried layer
$z = L_{\text{dried}}$
Frozen layer
moving interface
$z = L_{froz}$
Heating plate

Figure 2

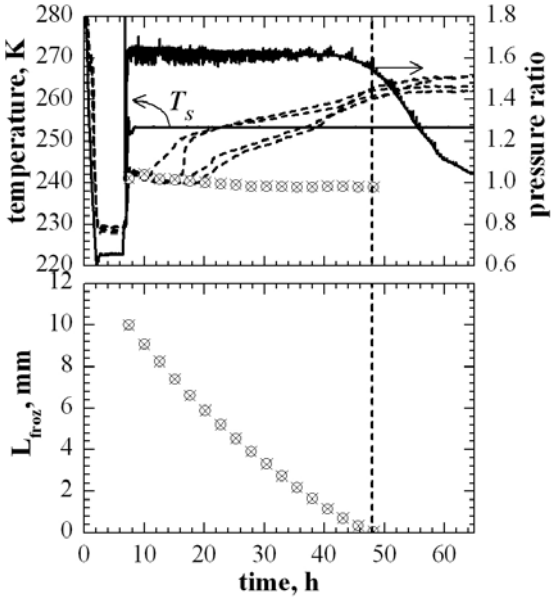

Figure 3

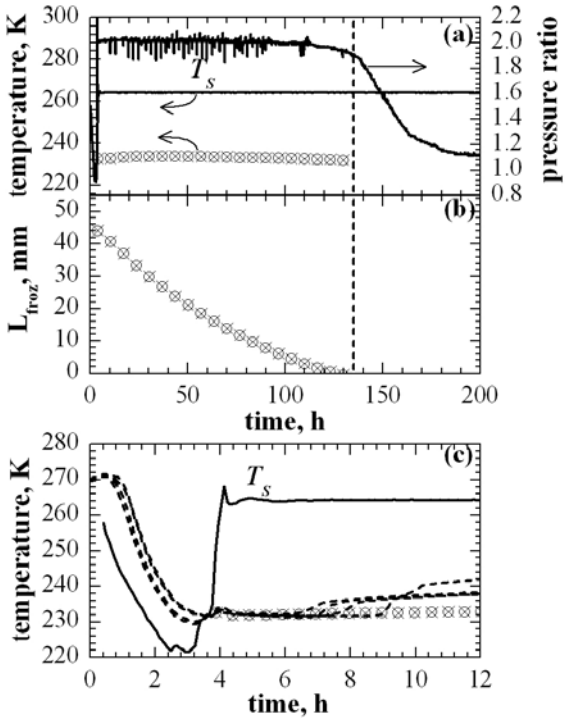

Figure 4

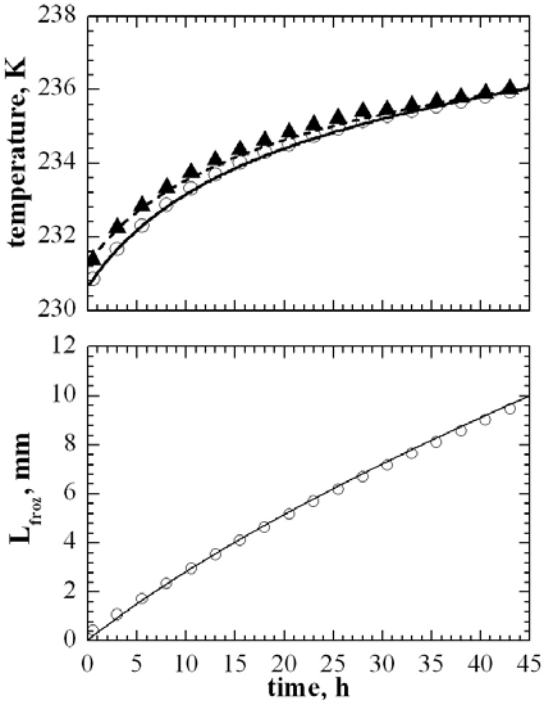
temperature, K
238
236
234
232
230
L_{froz}, mm
12
10
8
6
4
2
0
0
5
10
15
20
25
30
35
40
45
time, h

Figure 5

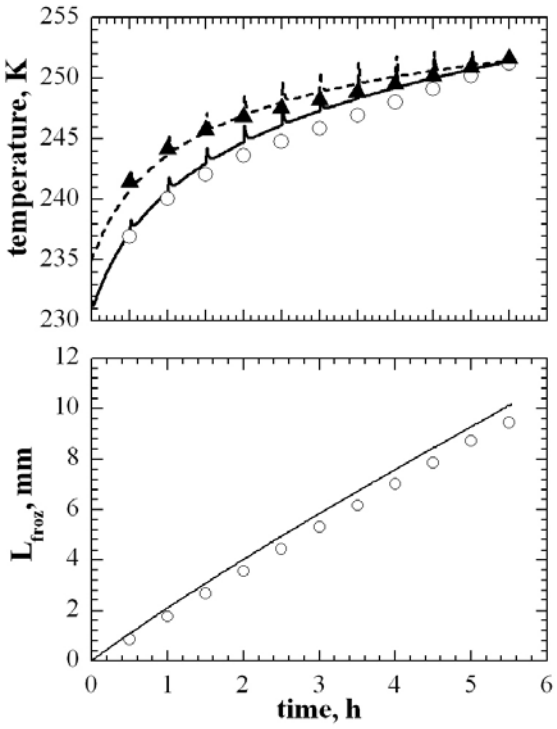
temperature, K
255
250
245
240
235
230
L_{froz}, mm
12
10
8
6
4
2
0
0
1
2
3
4
5
6
time, h

Figure 6

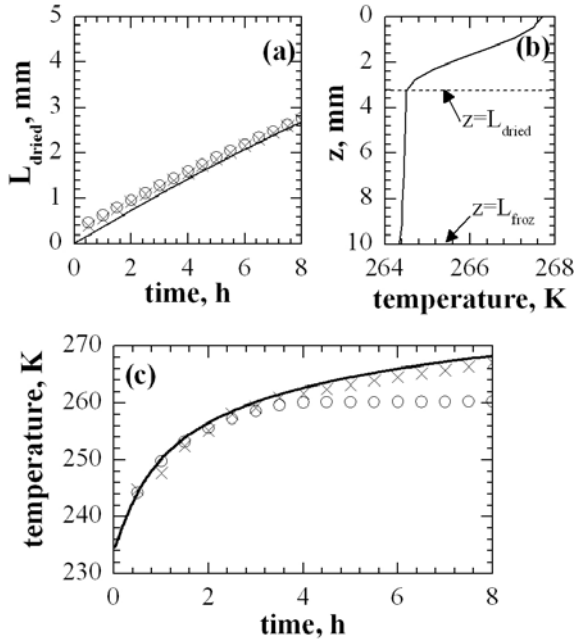
(a)
L_{dried}, mm
time, h
(b)
z, mm
$z=L_{dried}$
$z=L_{froz}$
temperature, K
(c)
temperature, K
time, h

Figure 7